Tidal dissipation within an elongated asteroid with satellite, and application to asteroid (216) Kleopatra

Gérard Caudal

Tidal dissipation within an elongated asteroid with satellite, and application to asteroid (216) Kleopatra

By Gérard CAUDAL

LATMOS/IPSL, UVSQ Université Paris-Saclay, Sorbonne Université, CNRS, Guyancourt, France

Submitted to ICARUS (january 2023)

Accepted (April 27th, 2023)

Abstract.

(216) Kleopatra is a highly elongated dumbbell shaped asteroid, which is spinning rapidly (spin period 5.38 hours), and has two satellites. The tidal migration rate of its outer satellite (related to asteroid tidal despinning) has been measured by Broz et al. (2021), and is used here to deduce the elastic properties of the asteroid, in particular its rigidity μ. For this purpose the satellite is modeled as an homogeneous elongated axisymmetric body, whose shape is described either as a cylinder or more realistically as a dumbbell. Such model asteroid is regarded as a beam (or rod) that undergoes tidal disturbances from the satellite. Due to the deformability of the asteroid, the tidal stresses produced within the body rise a compression tide in the direction of the asteroid's long axis, and a bending tide in the perpendicular direction. We compute the tidal amplitude of the total elastic energy stored within the asteroid, as a function of Young's modulus E. Provided that the tidal quality factor Q is known, this permits to deduce the power tidally dissipated within the asteroid. This is compared to the tidal dissipation deduced from Broz et al.'s (2022) observations of the tidal migration of Kleopatra's outer satellite. This permits to deduce the asteroid's Young's modulus E (or equivalently the rigidity μ through $\mu \approx E/(2.6 \pm 0.1)$). Using our dumbbell model for Kleopatra, we obtain a rigidity $\mu \approx 1.94 \times 10^7$ Pa if one assumes $Q \approx 40$, or $\mu \approx 1.40 \times 10^7$ Pa if one assumes $Q=100$. Such tidal dissipation is found to be more than 2 orders of magnitude higher than the tidal dissipation which would occur in a hypothetical spherical asteroid of same density and rigidity as Kleopatra, with radius equal to the volume equivalent radius ($R_V \approx 59.1$ km). Among model asteroids with same long axis length as Kleopatra ($2L \approx 267$km), dissipation is also found to be strongly dependent upon the shape of the asteroid (dumbbell, cylinder, or ellipsoid). Here the asteroid is regarded as an elastic solid, whereas it is presumably a weak rubble pile medium. The formalism developed here is however relevant provided that the asteroid may be regarded as a Maxwell material, because tidal frequencies are expected to be much higher than the inverse Maxwell time.

1. Introduction

Asteroid (216)Kleopatra presents several striking peculiarities. Firstly it is extremely elongated, in such a way that its shape resembles the «dumbbell » equilibrium shapes studied by Descamps (2015). Computing the effective potential including gravity and rotation, Marchis et al. (2021) have shown that Kleopatra's shape extends to a distance that is very close to the critical L1 equipotential. Another peculiarity is that Kleopatra possesses two identified satellites on close orbits. Broz et al. (2022) have been able to measure an increase of the period P_2 of the outer satellite Alexhelios, with a rate $\dot{P}_2=(1.8\pm0.1)\text{x}10^{-8}\text{dd}^{-1}$, and attributed it to the effect of tidal dissipation within Kleopatra produced by that satellite. Assuming a tidal quality factor Q≈40, which is typical for rubble pile asteroid, they found that the rate of increase of the satellite's rotation period was consistent with a Love number k_2≈0.3. As noticed by Broz et al. (2022), for uniform and spherical bodies, the Love number is related to the material rigidity μ of the asteroid through (Goldreich and Sari, 2009) :

$$\mu = \left(\frac{3}{2k_2} - 1\right)\frac{6}{19}\frac{GM^2}{R^2 S_O} \qquad (1)$$

where μ is the material rigidity, M, R and S_O are mass, radius and surface area of the asteroid, and G (=6.672x10^{-11} m^{3}kg^{-1}s^{-2}) is gravitational constant.

From this equation, taking R as the maximal radius R≈135km for Kleopatra, they obtained μQ≈2.7x10^7 Pa.

On another side, Marchis et al. (2008) reported that μ≈10^{8}Pa is a typical value for a moderately fractured asteroid, and μ>10^{10}Pa for consolidated rocky material. Assuming Q≈100 from Yoder (1982), they concluded that μQ can be in a large range from 10^{10} to 10^{12} Pa. Then by computing the evolution time scales of the most documented binary asteroid systems, and comparing them to the age of the solar system as an upper limit (4.5 Gyears), they were able to reduce that range, and concluded that μQ≈10^{10}Pa should be a realistic value for these binary systems.

The estimate μQ≈2.7x10^7 Pa by Broz et al. (2022) is therefore about three orders of magnitude smaller than the estimate μQ≈10^{10} Pa proposed by Marchis et al. (2008) for 100 km asteroids.

This paper is an attempt to go further in the comparison between the inferred elastic properties of Kleopatra with what is usually expected for 100 km asteroids, by revisiting the relation between Love number and rigidity for the specific case of a highly elongated asteroid such as Kleopatra.

In our formalism, we will follow the usual approach by considering the asteroid as an elastic solid. It should be pointed out, however, that such an object is not meant to be truly solid, but should be regarded as a weak medium consisting presumably of a pile of rubble. Dissipation in these weak media is not determined by their rigidity, but rather by their viscosity. The formalism developed here is however relevant provided that the asteroid can be considered as a Maxwell material and for frequencies well above the inverse of Maxwell time. This point will be discussed in the conclusion.

2. Interaction between a rigid elongated asteroid and its satellite :

As shown by Marchis et al. (2021), a visual inspection of the global shape of Kleopatra shows a very elongated object, with the presence of two lobes separated by a neck, resulting in a dumb-bell appearance. In this paper we will simplify the problem by considering the asteroid

as an homogeneous beam, or rod, whose model geometry will be presented below. The asteroid is spinning at angular frequency Ω. The satellite will be supposed to be on a circular orbit, in the plane perpendicular to the spin axis of the asteroid. The principal characteristics of the triple system involving Kleopatra and its two moons, are given in **Table 1**. Due to elasticity of the asteroid's material, the varying gravity force exerted by the satellites will produce both radial and azimuthal distortions of the asteroid. However, in this section 2, the asteroid will be regarded as a perfectly rigid body.

Here we consider only the interaction of Kleopatra with its outer satellite, which is the only one whose orbital period secular variation $\dot{P}_2$ has been measured by Broz et al. (2022). It is assumed that the presence of the inner satellite does not influence the observed $\dot{P}_2$. This is justified only on condition that there is no secular interaction between both satellites. It turns out that the ratio between orbital periods is $P_2/P_1 \approx 1.507$, which is close to the the 3:2 mean motion resonance. If both satellites were locked by resonance, tides would act on both moons together by imposing $\dot{P}_2 = 1.5\dot{P}_1$, and this would invalidate the relation between $\dot{P}_2$ and asteroid rigidity determined in this paper. However, according to numerical tests performed by Broz et al. (2021), the critical angle of the 3:2 mean motion resonance is not expected to librate, because orbits are much perturbed by the multipoles of Kleopatra and eccentricities are too small. Thus the assumption made in this paper that the inner satellite does not influence the observed $\dot{P}_2$ appears to be justified. In section 7.4 below, however, the situation of an hypothetical 3:2 mean motion resonance between both satellites will also be addressed.

2.1. Model geometry of the asteroid :

Two types of model geometry are used in this paper, which will be referred as the cylinder model, and the dumbbell model.

a). Cylinder model :
In the first approach, the asteroid is modeled as a right elliptic cylinder with uniform density, centered in O. The asteroid is spinning around the $O\vec{z}$ axis with angular velocity Ω. The body frame will be named ($O\vec{x}$, $O\vec{y}$, $O\vec{z}$), with long axis directed along the x direction. The right section of the cylinder is an ellipse with semi-axes R_y and R_z along the y and z directions. The parameters are determined from Marchis et al.'s (2021) MCPD model. Thus the length of the cylinder is taken as 2L=267km, and the values of R_y and R_z are adjusted to be consistent with mass (M= 2.97×10^{18}kg) and density (τ=3430 kg m^{-3}) of the asteroid (see **Table 1**), with the constraint that R_y/R_z=1.3 from MCPD model. This gives R_y=36.6 km and R_z= 28.2 km.

b). Dumbbell model :
The cylindrical model described above is a coarse approach of the asteroid shape. In order to get a more realistic picture, our dumbbell model consists in giving up the cylindrical approach, by modulating the semi-axes R_y and R_z , which then become functions of x. In order to simulate the dumb-bell configuration of the asteroid, the following functional form is chosen :

$$R_y(x) = R_{yO}\left[1 - \varepsilon\left\{1 + cos\left(\frac{3\pi}{2}\frac{x}{L}\right)\right\}\right] \quad ; \quad R_z(x) = R_{zO}\left[1 - \varepsilon\left\{1 + cos\left(\frac{3\pi}{2}\frac{x}{L}\right)\right\}\right] \qquad (2)$$

A realistic value for the modulation parameter ε is chosen as ε=0.13. Here again, the values of R_{yO} and R_{zO} are adjusted to be consistent with mass and density of the asteroid given in **Table 1**, with the constraint that R_y/R_z=1.3 from MCPD model. This gives R_{yO}=40.6 km and R_{zO}=

31.2 km. The resulting model asteroid shape is shown in **Figure 1**. It exhibits two symmetrical lobes, with a neck in the middle of the asteroid.

2.2. Gravitational potential produced by the satellite :

The satellite, assumed to be rotating on a circular orbit in the $(O\vec{x}, O\vec{y})$ plane, exerts a gravitational torque on the asteroid. In response to this torque, the asteroid undergoes a libration in azimuth.

A schematic view of the asteroid (here modeled as a cylinder) and its satellite is shown in **Figure 2**. The tidal gravitational potential exerted by the satellite S on a point P within the asteroid is given as (e.g., Murray and Dermott, 1999, p. 133)

$$U = -\beta r^2 \frac{3cos^2\psi - 1}{2} = -\beta r^2 \frac{3\cos(2\psi)+1}{4} \quad , \; with \quad \beta = \frac{Gm_2}{a_2^3} \tag{3}$$

where r=OP is distance of point P from center O of asteroid, Ψ is the angle $(\vec{OP}, \vec{OS})$, m_2 and a_2 are mass and semi-major axis of the satellite, respectively, and G is gravitational constant.

In the body frame $\left(O\vec{x}, O\vec{y}, O\vec{z}\right)$, let (r,θ,φ) be the polar coordinates of P, and (a_2, π/2, χ') the polar coordinates of satellite S. From equation (3) one deduces :

$$\begin{aligned}
\frac{\partial U}{\partial r} &= -\beta r\left[\frac{3}{2}sin^2\theta(1 + cos2(\chi' - \varphi)) - 1\right] \\
\frac{\partial U}{\partial \theta} &= -\frac{3}{4}\beta r^2[1 + cos2(\chi' - \varphi)]sin2\theta \\
\frac{\partial U}{\partial \varphi} &= -\frac{3}{2}\beta r^2 sin^2\theta \; sin2(\chi' - \varphi)
\end{aligned} \tag{4}$$

Ignoring the terms that do not depend upon time, we may also express the components of the gradient of U in the cartesian coordinates :

$$\begin{aligned}
(\nabla U)_x &= \frac{3}{2}\beta[-xcos2(\chi' - \varphi) + ysin2(\chi' - \varphi)] \\
(\nabla U)_y &= -\frac{3}{2}\beta[ycos2(\chi' - \varphi) + xsin2(\chi' - \varphi)] \\
(\nabla U)_z &= 0
\end{aligned} \tag{5}$$

2.3. Inertial acceleration due to azimuthal libration :

As mentioned above, in this section 2 the asteroid is considered as a perfectly rigid body. We first define the rotating reference frame $\left(O\vec{X}, O\vec{Y}, O\vec{Z}\right)$, with units vectors $(\vec{e}_X, \vec{e}_Y, \vec{e}_Z)$, which is spinning around axis $O\vec{Z}$ at the uniform rate Ω with respect to the inertial frame. In this rotating reference frame, the material located at point (X, Y, Z) of the asteroid undergoes the inertial centrifugal acceleration $\Omega^2(X\vec{e}_X + Y\vec{e}_Y)$. This acceleration is dominant over all other inertial accelerations, but it is independent on time, and therefore does not produce time dependent stresses. The force that it generates is balanced principally by self-gravity, although the shape of the surface may also be affected by a number of physical effects involving internal friction, constitutive laws and cohesive forces (Scheeres, 2010; Descamps, 2015, 2016).

Superimposed on that constant acceleration, the gravitational torque exerted by the satellite is time dependent and this produces a libration of the asteroid about axis $O\vec{Z}$. To account for this libration, we define the body frame $(O\vec{x}, O\vec{y}, \vec{Oz})$, which is librating with respect to the rotating reference frame (with $\vec{Oz} \equiv \vec{OZ}$).

Let χ be the azimuth of the satellite in the rotating reference frame $\left(O\vec{X}, O\vec{Y}, \vec{OZ}\right)$. Since the satellite orbit is assumed circular, the angle χ varies linearly with time, according to $\chi=(n_2-\Omega)t = -(\omega_S/2)t$, where ω_S is the semi-diurnal tidal angular velocity. Let us define the libration angle ξ as the azimuthal deviation of the asteroid long axis $\vec{Ox}$ from the reference axis $\vec{OX}$. Then, in the body frame $(O\vec{x}, O\vec{y}, \vec{Oz})$, the azimuth of the satellite is $\chi' = \chi - \xi$ (see **Figure 2**). The libration of the asteroid is governed by the equation of motion (e., g., Goldreich and Peale, 1966) :

$$\ddot{\xi} = +\frac{3}{2}\beta\lambda \sin(-\omega_S t) \quad ; \quad where \quad \lambda = \frac{(B-A)}{C} = \frac{\iiint (x^2-y^2)dxdydz}{\iiint (x^2+y^2)dxdydz} \qquad (6)$$

where A<B<C are the inertial moments about axes $O\vec{x}, O\vec{y}, \vec{Oz}$, respectively, and the integrals are performed over the volume of the asteroid. From the parameter set of **Table 1** describing asteroid (216) Kleopatra, one gets λ=0.893 for the cylinder model, or λ=0.896 for the dumbbell model.

Equation (6) describes a forced harmonic oscillator and, since the averages of $\dot{\xi}$ and ξ must be 0, we get :

$$\dot{\xi} = +\frac{3}{2}\frac{\beta\lambda}{\omega_S}\cos(-\omega_S t) \quad ; \quad \xi = -\frac{3}{2}\frac{\beta\lambda}{\omega_S^2}\sin(-\omega_S t) \qquad (7)$$

With the parameters of **Table 1**, this gives an amplitude of libration ξ_O=5.39x10^{-7} rad. This value is so low that in practice, in equations (5), the angle $\chi'=\chi-\xi$ may be replaced by χ without significantly modifying the result.

In the body reference frame, the libration produces an inertial acceleration $\vec{\Gamma_L} = -r\,sin\theta\,\ddot{\xi}\,\vec{e_\varphi}$, where $\vec{e_\varphi}$ is the azimuthal unit vector in the local frame. $\vec{\Gamma_L}$ may also be written in the cartesian frame :

$$(\Gamma_L)_x = \frac{3}{2}\beta\lambda\, y\, sin(-\omega_S t)$$
$$(\Gamma_L)_y = -\frac{3}{2}\beta\lambda\, x\, sin(-\omega_S t)$$
$$(\Gamma_L)_z = 0 \qquad (8)$$

In addition, since the reference frame is spinning about axis $\vec{OZ}$, any element of matter undergoes the inertial Coriolis acceleration $\vec{\Gamma}_{Cor} = -2\vec{\Omega}\times\vec{V}$, where $\vec{V}$ is its velocity relative to the rotating reference frame. From equation (7), it may be seen that the amplitude of $\dot{\xi}$ is $\dot{\xi}_O = 3\beta\lambda/2\omega_S \approx$3x10^{-10} rad/s , and thus $\dot{\xi}_O/\Omega \approx 10^{-6}$. Thus the Coriolis acceleration in the body (librating) frame and in the reference frame do not differ appreciably. Thus in the body frame $\vec{\Gamma}_{Cor}$ may be written :

$$(\Gamma_{Cor})_x = +3\beta\lambda\frac{\Omega}{\omega_S}x\cos(-\omega_S t)$$
$$(\Gamma_{Cor})_y = +3\beta\lambda\frac{\Omega}{\omega_S}y\cos(-\omega_S t)$$
$$(\Gamma_{Cor})_z = 0 \qquad (9)$$

In the body frame, the net acceleration undergone by any element of matter within the asteroid, is then (ignoring terms that do not depend upon time):

$$\vec{\Gamma} = (-\nabla U) + \vec{\Gamma}_L + \vec{\Gamma}_{Cor} \qquad (10)$$

The cartesian components of $(-\nabla U)$ may be taken from equation (5), and we recall that $2\chi' \approx 2\chi = (-\omega_S t)$.

For example, for the dumbbell model, for $\theta=\pi/2$ and $\varphi=0$ we get $(\Gamma_L)_y/(-\nabla U)_y = -\lambda = -0.896$ for $\chi=\pi/4$, and $(\Gamma_{Cor})_x/(-\nabla U)_x = 2\lambda\Omega/\omega_S = 0.976$ for $\chi=0$. Thus, even though the amplitude ξ_O of the libration angle ξ is extremely small, it is clear that the inertial accelerations $\vec{\Gamma}_L$ and $\vec{\Gamma}_{Cor}$ due to libration introduce significant corrections to the gravitational acceleration.

3. Normal stress and bending moment for an elastic solid beam (static approach)

The asteroid is now regarded as a solid elastic beam, which is subject to variable normal stress as well as shear stress due to the presence of the gravitational forces produced by the satellite. In this section we assume that the frequencies of gravitational excitations of the asteroid by the satellite are much slower than the natural frequencies of the asteroid. Therefore a static approach is taken here. The oscillatory behaviour of the system will be addressed in the next sections. Three main modes of oscillation will be addressed : longitudinal strain in the x direction, longitudinal strain in the y direction, and bending in the y direction.

3.1. Strain energy due to normal stress in the x direction:

We use the body frame (Oxyz), and we consider the slice at abscissa x, where one defines the average normal stress

$$\sigma = \frac{F_x}{S} \qquad (11)$$

where F_x is the axial tensile load, and $S(x)=\pi R_y R_z$ is the area of the beam cross section at abscissa x. Let $u_x(x)$ be the longitudinal elastic displacement. From Hooke's law, the longitudinal strain ε_x at abscissa x is given by (Slaughter, 2002) :

$$\varepsilon_x = \frac{du_x}{dx} = \frac{\sigma}{E} = \frac{F_x}{SE} \qquad (12)$$

where E is Young's modulus. The normal force per unit length produced at abscissa x is given by

$$w_x(x) = \rho\iint_{y,z}\Gamma_x dydz \qquad (13)$$

where ρ is asteroid density, and integration is carried out over the cross section of the beam. If axis $\overrightarrow{Ox}$ is oriented from left to right, the normal force exerted on the right-hand side of an infinitesimal slice at abscissa x is then:

$$F_x(x) = \int_{x_1=x}^{L} w_x(x_1)dx_1 \qquad (14)$$

Note that a similar force $F'_x(x) = \int_{x_1=-L}^{x} w_x(x_1)dx_1$ is exerted on the left-hand side of the same slice. Due to the symmetry of the asteroid and of the semi-diurnal tide, one has $F'_x(x) = -F_x(x)$, so that the total force on the slice is zero, but the material within the slice is compressed by the antagonist forces $F_x(x)$ and $F'_x(x)$.

Solving the integration over z, equations (12), (13), and (14) finally give :

$$F_x(x) = SE\frac{du_x}{dx} = \rho \int_{x_1=x}^{L} \left[\int_{y=-R_y(x_1)}^{R_y(x_1)} 2R_z(x_1)\sqrt{1-\frac{y^2}{R_y^2(x_1)}}\,\Gamma_x dy \right] dx_1 \qquad (15)$$

The asteroid and the semi-diurnal gravitational forces are symmetric with respect to origin. The strain energy stored within the half beam 0≤x≤L is half the total strain energy E_{Sx}, and is given as (Stokey, 2002) :

$$\frac{1}{2}E_{Sx} = \frac{E}{2}\int_0^L S\left(\frac{du_x}{dx}\right)^2 dx \qquad (16)$$

From equation (12) this may also be written, for the entire symmetric beam (-L≤x≤L) :

$$E_{Sx} = E\int_0^L S(x)\left(\frac{du_x}{dx}\right)^2 dx = \frac{1}{E}\int_0^L \frac{F_x^2(x)}{S(x)}dx \qquad (17)$$

3.2. Strain energy due to normal stress in the y direction :

In this section, the same approach as section 3.1 is used, except that the strain and stress in the y direction, instead of x direction, are addressed. Inverting the roles of x and y, we may compute the normal force F_y exerted on the slice performed at ordinate y:

$$F_y(y) = \rho \int_{y_1=y}^{R_{yO}} \left(\int_{x=-L}^{L} 2R_z(x)\sqrt{Max\left[\left(1-\frac{y_1^2}{R_y^2(x)}\right),\,0\right]}\,\Gamma_y(x,y_1)dx \right) dy_1 \qquad (18)$$

where R_{yO} is the reference radius of the dumbbell model in the direction y, given in **Table 1.** Note that, contrary to equation (15), the double integral in equation (18) is performed first over y_1, then on x. This requires the introduction of $Max\left[\left(1-y_1^2/R_y^2(x)\right),0\right]$ in equation (18) for the dumbbell model, to ensure that integration is limited to the interior of the asteroid ($|y_1| \le R_y(x)$).

Due to the symmetry of the asteroid with respect to origin, and symmetry of semi-diurnal gravitational forces, the component Γ_y verifies the following symmetry property :

$$\Gamma_y(-x,y) = -\Gamma_y(x,-y) \qquad (19)$$

This permits to reduce the integration over x to the 0≤x≤L interval. Applying the adequate changes of variables, we get :

$$F_y(y) = 2\rho \int_{y_1=y}^{R_{yO}} \left(\int_{x=0}^{L} R_z(x) \sqrt{Max\left[\left(1 - \frac{y_1^2}{R_y^2(x)}\right), 0\right]} \left(\Gamma_y(x, y_1) - \Gamma_y(x, -y_1)\right) dx \right) dy_1 \quad (20)$$

Similarly as was done in section 3.1, one can compute the compressional strain energy stored in the whole asteroid :

$$E_{Sy} = \frac{1}{2E} \int_{-R_y}^{R_y} \frac{F_y^2(y)}{S\prime(y)} dy \quad (21)$$

where S'(y) is the area of the slice performed at ordinate y. For the dumbbell model, the slice at ordinate y is not necessarily a connected surface, but in any case S' is given as

$$S'(y) = 4 \int_{x=0}^{L} R_z(x) \sqrt{Max\left[\left(1 - \frac{y^2}{R_y^2(x)}\right), 0\right]} \, dx \quad (22)$$

Comparison between the compressional strain energies E_{Sx} and E_{Sy} stored in the x and y directions respectively may be done from equations (17) and (21). The ratio $q=E_{Sy}/E_{Sx}$ was computed for model asteroids with the same mass and density as Kleopatra, but with the asteroid length 2L along the x axis taken as a free parameter (the radii R_{yO} and R_{zO} are modified accordingly to preserve volume). In **Figure 3**, the ratio $q=E_{Sy}/E_{Sx}$ is plotted as a function of the triaxiality $\lambda=(B-A)/C$, for both types of asteroid (cylinder, or dumbbell). It can be seen that q is slightly higher for cylinder model than for dumbbell model (by a factor of 1.4 to 1.8). In both cases, while q is of the order of unity for poorly elongated asteroids ((B-A)/C<<1), it drops dramatically to less than 10^{-6} for Kleopatra's geometry ((B-A)/C=0.896 in the dumbbell model, corresponding to L=133.5 km). Compressional strain energy in the y direction is thus insignificant for Kleopatra. Henceforth in this paper, unless otherwise specified, the compressional strain in the y direction, and compressional strain energy E_{Sy} , will therefore be neglected.

3.3. Strain energy due to shear bending :

Due to gravitational interaction with the satellite, the asteroid will also undergo bending in the y direction. When an external force vector $\vec{F}$ is acting at a point A in the asteroid (see **Figure 4**), the bending moment produced by $\vec{F}$ about the axis parallel to $\overrightarrow{Oz}$ that passes through a reference point Q located on the x axis is defined as :

$$M_z = \left(\overrightarrow{QA} \times \vec{F} \right) . \overrightarrow{e_z} \quad (23)$$

Where $\overrightarrow{e_z}$ is the unit vector along $\overrightarrow{Oz}$.

Components of the external elementary force $\overrightarrow{dF}$ exerted at point A, the bending moment produced at point Q may be written:

Within the asteroid, the elementary volume around the running point A produces a force and bending moment, and those are transmitted by the solid body to point Q. Thus if (x, 0, 0) and (x_1, y_1, z_1) are the coordinates of points Q and A, respectively, and *(dF_x, dF_y, dF_z)* the components of the external elementary force $\overrightarrow{dF}$ exerted at point A, the bending moment produced at point Q may be written:

$$dM_z = (x_1 - x)dF_y - y_1 dF_x \tag{24}$$

The total bending moment produced at point Q by the component F_y may be obtained by integrating the first term of the right hand side of equation (24) over all running points A. This gives:

$$M_{yz}(x) = \int_{x_1=x}^{L} \left[(x_1 - x)w_y(x_1)\right] dx_1 \tag{25}$$

Where $w_y(x_1)$ is the force per unit length produced at abscissa x_1 by the y component of acceleration :

$$w_y(x_1) = \rho \iint_{y,z} \Gamma_y(x_1, y, z) dydz \tag{26}$$

Note that the dummy integration variables in equation (26) have been named y and z in order to simplify scripture, even though they represent coordinates y_1 and z_1 of running point A. The integration is done over the cross section of the asteroid at abscissa x_1. Performing the integration over z, we can then write :

$$M_{yz}(x) = \rho \int_{x_1=x}^{L} \int_{y=-R_y(x)}^{R_y(x)} 2R_z(x) \sqrt{1 - \frac{y^2}{R_y^2(x)}}\ (x_1 - x)\Gamma_y \mathrm{d}y\mathrm{d}x_1 \tag{27}$$

Similarly the x component of the external force (second term of the right hand side of equation (24)) produces a bending moment M_{xz} at point Q, and the total bending moment M_z=M_{xz}+M_{yz} finally reads :

$$M_z(x) = \rho \int_{x_1=x}^{L} \int_{y=-R_y(x)}^{R_y(x)} 2R_z(x) \sqrt{1 - \frac{y^2}{R_y^2(x)}}\ \left[(x_1 - x)\Gamma_y - y\Gamma_x\right] dydx_1 \tag{28}$$

At abscissa x, let u_B(x) be the bending displacement along y, and let $\gamma(x) \approx du_B/dx$ be the distortion angle between the asteroid's axis and $\overrightarrow{Ox}$. The deflection u_B is related to the bending moment and the Young modulus through (Slaughter, 2002) :

$$\frac{d^2u_B}{dx^2} = \frac{d\gamma}{dx} = \frac{M_z(x)}{EI} \quad (29)$$

where the beam area moment of inertia I is given as

$$I = \iint y^2 dydz \quad (30)$$

The surface integral in equation (30) is performed over the asteroid section. For the elliptical section with semi-axes R_y and R_z , this gives $I = \frac{\pi}{4} R_z R_y^3$. For our dumbbell model, I is thus a function of x.

The strain energy of bending within the half beam (0≤x≤L) is (Stokey, 2002) :

$$\frac{1}{2} E_B = \frac{E}{2} \int_0^L I \left(\frac{d^2u_B}{dx^2}\right)^2 dx \quad (31)$$

From equation (29), this becomes, for the entire symmetric beam (-L≤x≤L) :

$$E_B = \frac{1}{E} \int_{x=0}^{L} \frac{M_z^2(x)}{I} dx \quad (32)$$

4. Natural frequencies of oscillations of the asteroid

In section 3, compression and bending were treated in a static approach. Since the gravitational excitation by the satellite is oscillatory, such approach may be justified only if the forcing frequency is small compared to the natural frequencies of the asteroid. It is therefore necessary to determine the natural resonance frequencies of the asteroid, with respect to both axial compression and bending. Exact solutions require solving intricate partial differential equations. However for most problems where only the fundamental natural frequency is needed, Rayleigh's method permits to find very good approximations of the natural frequencies (Stokey, 2002). The principle is to point out that, for a freely oscillating body, when the deflection from equilibrium is maximum, all parts of the body are motionless. At that time all the vibrational energy is in the form of elastic strain energy. Conversely, when the body is passing through its equilibrium position, all the energy is in the form of kinetic energy. For conservation of energy, both energies should be equal. Rayleigh's method consists in computing these maximum energies, equate them, and solve for frequency (Stokey, 2002). The natural frequencies will be given here only for compressional tide in the x direction, and for bending tide. For the sake of brevity is will not be given for compressional tide in the y direction, since the latter is negligible for Kleopatra, as seen in section 3.2.

4.1. Natural frequency for normal stress in the x direction :

If the excitation frequency is much lower than the asteroid natural frequencies, the results obtained in section 3 for strain energy in the static case are still valid here provided that the static quantities are replaced by peak values of oscillatory quantities. If E_{Kx} is the peak kinetic energy produced in the beam by longitudinal displacement along x, the peak kinetic energy for half beam (0≤x≤L) is given by (Stokey, 2002) :

$$\frac{1}{2} E_{Kx} = \frac{\rho}{2} \int_0^L S \left(\frac{du_x}{dt}\right)^2 dx \quad (33)$$

Thus for the entire symmetric beam oscillating freely at angular frequency ω_O :

$$E_{Kx} = \rho \int_0^L S\omega_{Ox}^2 u_x^2 dx \qquad (34)$$

The longitudinal displacement u_x is obtained from equation (12), together with the boundary condition $u_x(0)=0$, yielding :

$$u_x(x) = \frac{1}{E}\int_0^x \frac{F_x}{S} dx \qquad (35)$$

Equating energies E_{Sx} and E_{Kx} from equations (17) and (34), one gets:

$$\omega_{Ox}^2 = \frac{1}{\rho E}\frac{\int_0^L \frac{1}{S}F_x^2(x)dx}{\int_0^L S u_x^2(x)dx} \qquad (36)$$

4.2. Natural frequency for shear bending:

The same approach is used for the azimuthal distortion of the beam. The peak kinetic energy due to bending for half beam ($0 \le x \le L$) is similarly (Stokey, 2002):

$$\frac{1}{2}E_{KB} = \frac{\rho}{2}\int_0^L S\left(\frac{du_B}{dt}\right)^2 dx \qquad (37)$$

Equating again kinetic energy E_{KB} with strain energy E_B given by equation (32), one gets finally the natural angular frequency ω_{OB} for bending :

$$\omega_{OB}^2 = \frac{1}{\rho E}\frac{\int_0^L \frac{1}{I}M_z^2(x)dx}{\int_0^L S u_B^2(x)dx} \qquad (38)$$

To compute $u_B(x)$, one may first determine $\gamma(x)=du_B/dx$ by integrating equation (29). This gives :

$$\gamma(x) = \gamma_1(x) - \gamma_O \quad ; \quad where \quad \gamma_1(x) = \frac{1}{E}\int_0^x \frac{1}{I}M_z(x_1)dx_1 \qquad (39)$$

and γ_O is an integration constant to be determined.

A further integration, together with the boundary condition $u_B(0)=0$, permits to determine $u_B(x)$:

$$u_B(x) = \int_0^x (\gamma_1(x) - \gamma_O)dx \qquad (40)$$

In order to determine the integration constant γ_O , we note that, unlike libration, the elastic distortion of the asteroid is an internal process which does not involve exchange of angular momentum between the asteroid and the exterior. Thus at the time of maximum elongation $u_B(x)$, the asteroid has received no other angular momentum from the exterior than if it were a perfectly rigid body. Moreover, for any point on the x axis, u_x and u_B are in quadrature (this may be deduced from equation (10), and it will still be true when the Coriolis coupling

between u_x and u_B will be introduced in section 5 below). Thus at the time of maximum elongation $u_B(x)$, then $u_x(x,t)$ is zero. The condition that the average of maximum angular deviation (u_B/x) relative to rigid body is zero may then be written :

$$\int_0^L \rho x^2 \left(\frac{u_B}{x}\right) S dx = 0 \qquad (41)$$

or equivalently :

$$\int_0^L \rho S x u_B(x) dx = 0 \qquad (42)$$

Together with equation (40), this permits to determine the constant γ_O , given here, for homogeneous body (ρ=constant) :

$$\gamma_O = \frac{\int_0^L Sx\left(\int_0^x \gamma_1(x_1)dx_1\right)dx}{\int_0^L Sx^2 dx} \qquad (43)$$

In the case where the cross section area S were taken as uniform (cylindrical model asteroid), this expression could be simplified :

$$\gamma_O = \frac{3}{L^3}\int_0^L x\left(\int_0^x \gamma_1(x_1)dx_1\right)dx \qquad (44)$$

5. Coupling between bending and compression under Coriolis acceleration :

The expressions for accelerations Γ_x and Γ_y were given in section 2, including a first Coriolis term related to asteroid libration, given by equation (9). In addition, since the distortions of the asteroid vary with time, those also imply velocities with respect to the spinning frame, and thus additional Coriolis acceleration.
Explicitly writing the dependence with time, we may express the complex amplitudes $\hat{u}_x$ and $\hat{u}_y$ of the elastic displacement :

$$\hat{u}_x(x,y,t) = u_x(x)\, exp\left(i(-\omega_S t + \zeta_x)\right)$$
$$\hat{u}_y(x,y,t) = u_B(x)\, exp\left(i(-\omega_S t + \zeta_B)\right) \qquad (45)$$

The phases $\zeta_x(x)$ and $\zeta_B(x)$ of the oscillations of u_x and u_B will not be discussed here. We have neglected the compressional distortion related to normal displacement in the y direction, since it is insignificant for Kleopatra, as discussed in section 3.2.

By derivation, this implies :

$$\frac{d\hat{u}_x}{dt} = -i\omega_S u_x(x) exp\left(i(-\omega_S t + \zeta_x)\right) \;\; ; \;\; \frac{d\hat{u}_y}{dt} = -i\omega_S u_B(x) exp\left(i(-\omega_S t + \zeta_B)\right) \qquad (46)$$

Since ω_S is a semi-diurnal frequency, the azimuthal angle of the satellite is $\chi = -\omega_S t/2$. Equation (46) may thus be rewritten :

$$\frac{d\hat{u}_x}{dt} = \omega_S u_x(x) exp\left[i\left(2\chi - \frac{\pi}{2} + \zeta_x\right)\right] \;\; ; \;\; \frac{d\hat{u}_y}{dt} = \omega_S u_B(x) exp\left[i\left(2\chi - \frac{\pi}{2} + \zeta_B\right)\right] \qquad (47)$$

Denoting $\overrightarrow{V'} = d\vec{u}/dt$ the elastic displacement velocity vector, inertial Coriolis acceleration is $\overrightarrow{\Gamma'}_{Cor} = -2\vec{\Omega}\times\overrightarrow{V'}$. This gives :

$$[\Gamma'_{Cor}(x,\chi)]_x = +2\Omega\omega_S u_B(x,\chi-\pi/4)$$
$$[\Gamma'_{Cor}(x,\chi)]_y = -2\Omega\omega_S u_x(x,\chi-\pi/4)$$
$$[\Gamma'_{Cor}]_z = 0 \qquad (48)$$

and similarly :

$$[\Gamma'_{Cor}(x,\chi-\pi/4)]_x = -2\Omega\omega_S u_B(x,\chi)$$
$$[\Gamma'_{Cor}(x,\chi-\pi/4)]_y = +2\Omega\omega_S u_x(x,\chi)$$
$$[\Gamma'_{Cor}]_z = 0 \qquad (49)$$

This acceleration should be added to equation (10). It will produce coupling between the different modes of oscillation. In practice, since u_x and u_B are not known a priori, the model is first run with this second Coriolis term ignored, for both positions χ and (χ-π/4) of the satellite. Then it is run a second time with these corrections included, and the process is iterated. Convergence is virtually achieved after the third iteration.

6. Relation between orbital period rate and Young's modulus :

6.1. Amplitude of elastic energy stored by the forced oscillator

The amplitudes of the longitudinal and bending elastic energies E_{Sx} and E_B stored within the asteroid, given in equations (17) and (32), were obtained in a static approach, characterized by the assumption that the rate of variations are much slower than the natural frequencies of the asteroid. The tidal perturbation, on the other hand, produces a forced oscillation at the semi-diurnal angular rate $\omega_S=2(\Omega-n_2)$, which needs to be compared to the natural resonance rates of the asteroid. When the forcing rate ω_S becomes comparable to the resonance rate ω_O of an harmonic oscillator, then the amplitude of the energy stored by the forced oscillator in a static approach must be multiplied by a resonance factor, given as (see Appendix A):

$$K(\eta) = \frac{1}{(1-\eta^2)^2+\frac{\eta^2}{Q^2}} \qquad (50)$$

Where $\eta = \frac{\omega_S}{\omega_O}$, and Q is the quality factor of the harmonic oscillator. The resonance factor K varies between K≈1 in the static case (η<<1) and $K=Q^2$ at resonance (η=1).

The resonance angular rates ω_{Ox} and ω_{OB} were given respectively in equations (36) for compression oscillation along x, and (38) for bending oscillation. The maximum elastic energies actually stored within the asteroid must then be written :

$$E'_{Sx} = E_{Sx}\times K(\omega_S/\omega_{Ox}) \quad ; \quad E'_B = E_B\times K(\omega_S/\omega_{OB}) \qquad (51)$$

Similarly, the strain displacements $u_x(x)$ and $u_B(x)$ (see equations (35) and (40)) need to be multiplied by the square root of the resonance factor, and thus replaced respectively by :

$$h_x(x) = u_x(x)\times\sqrt{K(\omega_S/\omega_{Ox})} \quad ; \quad h_B(x) = u_B(x)\times\sqrt{K(\omega_S/\omega_{OB})} \qquad (52)$$

6.2. Calculation of the rate of increase of orbital period :

By definition, the tidal quality factor Q may be written :

$$Q = \frac{2\pi E_O}{\Delta E} \qquad (53)$$

where ΔE is the energy dissipated over one cycle, and E_O is the peak elastic energy stored during the semi-diurnal cycle. In the problem treated here, there are actually two tides : the bending tide and the compressional tide, and there is a phase shift of $\pi/2$ between the time variation of the bending tide and compressional tide (corresponding to a shift of $\pi/4$ of the satellite azimuth χ). If we assume that the tidal oscillations are linear, the effects of bending and compressional tides can be calculated separately and then simply added.

The rate of tidal energy dissipation $\dot{E}_T$ within the asteroid is equal to $\Delta E/T_S$, where $T_S=2\pi/\omega_S$ is the tidal period. Thus equation (53) gives :

$$\dot{E}_T = -\frac{\omega_S(E'_{Sx}+E'_B)}{Q} \qquad (54)$$

where the amplitudes of the longitudinal and bending energies E'_{Sx} and E'_B are given in equations (51).

The rate of tidal energy dissipation in the asteroid may also be expressed as a function of the migration rate of the satellite (Murray an Dermott, 1999, p. 163) :

$$\dot{E}_T = -\frac{1}{2}\frac{Mm_2}{(M+m_2)} n_2 a_2 \dot{a}_2 (\Omega - n_2) \qquad (55)$$

Note that equation (55) implicitly assumes that the moment of inertia of the asteroid is independent on Ω (an assumption which is also done here). From third Kepler's law, $\dot{a}_2/a_2 = -(2/3)(\dot{n}_2/n_2) = (2/3)\dot{P}_2/P_2$. Eliminating $\dot{E}_T$ from equations (54) and (55), using third Kepler's law, and accounting that $m_2 \ll M$, we get the orbital period rate :

$$\dot{P}_2 = \frac{6P_2(E'_{Sx}+E'_B)}{a_2^2 m_2 n_2 Q} \qquad (56)$$

From equations (17) and (32), one sees that amplitudes of elastic energies E_{Sx} and E_B are dependent upon Young's modulus E. Assuming a value for quality factor Q, measurement of orbital period rate $\dot{P}_2$ may thus be used to determine Young's modulus E, obtained implicitly through equation (56).

7. Results

7.1. Kleopatra's rigidity μ inferred from period migration rate $\dot{P}_2$

Three parameters are relevant to describe the elastic properties of a material. Those are (i) Young's modulus E which has been used up to now in the paper, (ii) shear modulus or rigidity μ, and (iii) Poisson's ratio ν. These are however not independent since they are linked by the relation $E=2(1+\nu)\mu$. Moreover the value of Poisson ratio ν is fairly well constrained for fractured rocky material. The estimates of Poisson ratio performed by Davy et al. (2018) for fractured rock masses span a narrow interval between 0.25 and 0.35. We will take here an intermediate estimate $\nu \approx 0.3 \pm 0.05$ so that the ratio $E/\mu = 2(1+\nu) \approx 2.6 \pm 0.1$. Since most often it is the rigidity μ that is used to describe the elastic properties of planetary material, we will take $E/\mu \approx 2.6$, and present the results below in terms of rigidity μ, in order to make comparison easier with other bodies.

The value of the quality factor Q for an asteroid of the size of Kleopatra is rather uncertain. Goldreich and Sari (2009) propose $Q \approx 100$ for monoliths, but point out that Q may be much lower for a rubble pile. Broz et al. (2022) assume $Q \approx 40$ on the basis that Kleopatra is an irregular body close to critical rotation. For running the model here we will use two alternative hypotheses : Q=40 and Q=100.

Figure 5 displays the value of the computed migration period rate $\dot{P}_2$ as a function of rigidity μ for the dumbbell model. Here a quality factor Q=40 is taken. It is seen that both compressional strain and bending strain contribute significantly to the migration period rate (and thus to dissipation). The bending tide dominates for low values of μ, while the compressional tide dominates for high values of μ. The computed total period rate matches the rate measured by Broz et al. (2022) ($\dot{P}_2 = 1.8 \times 10^{-8}$ day/day) for $\mu \approx 1.94 \times 10^7$ Pa. This situation is reasonably far from resonance, since it gives $\omega_S/\omega_{oB} \approx 0.205$ and $\omega_S/\omega_{Ox} \approx 0.476$. From equation (50) this gives resonance factors $K(\eta) = 1.09$ and 1.67, respectively. Similar curves (not shown) obtained assuming Q=100, would match modeled and observed $\dot{P}_2$ for $\mu \approx 1.40 \times 10^7$ Pa. This gives a tidal parameter $\mu Q \approx 7.8 \times 10^8$ Pa for Q=40, or $\mu Q \approx 1.40 \times 10^9$ Pa for Q=100. Marchis et al. (2008) proposed $\mu Q \approx 10^{10}$ Pa as a realistic value. The values inferred here are therefore 7 to 13 times lower than the value they proposed.

In order to account for the elongated nature of the asteroid, Broz et al. (2022) proposed to apply the tidal theory of a spherical body (equation (1)), but replacing the volume equivalent radius by the maximal radius. Assuming $Q \approx 40$, they inferred $\mu Q \approx 2.7 \times 10^7$ Pa, which is still 29 times smaller than the value inferred in this paper.

7.2. Compressional and bending distortion as function of distance from center

Figure 6 shows the amplitude of the distortions h_x and h_B, defined in equation (52), as a function of distance along x axis. The maximum bending distortion h_B is attained for $\chi = \pm 45°$ (modulo 180°), and its amplitude is of the order of ±2cm. Similarly, the maximum compression distortion h_x along x is attained for $\chi = 0°$ (modulo 180°), and its amplitude is of the order of ±4cm. Since the bending distortion h_B is along the y direction, the curve representing h_B in **Figure 6** also represents the shape of the distorted longitudinal axis of the asteroid, with coordinate y magnified by a factor of about 2.5×10^6.

7.3. tidal dissipation in a non-spherical body as a function of shape :

The model presented in this paper was built to describe specifically the situation of a highly elongated asteroid, which permitted us to model the asteroid as a beam which is stressed by bending and compression. It is thus not supposed to describe the situation of a body for which

the 3 dimensions would be of comparable length. It may however be instructive to apply the model to prolate bodies of arbitrary triaxiality λ=(B-A)/C, in order to try to bridge the gap between the classical approach of a spherical asteroid and the present approach. For this reason, as was done in **Figure 3** above, the dissipated power was computed for model asteroids with the same mass and density as Kleopatra, but with the asteroid length 2L along the x axis taken as a free parameter (the radii R_{yO} and R_{zO} are modified accordingly to preserve volume). For every value of the asteroid length 2L, the triaxiality λ=(B-A)/C can be computed numerically through equation (6). The relation between asteroid length and triaxiality is displayed in **Figure 7** for the dumbbell and cylinder models.

The dissipated power is compared to the power dissipated within a spherical asteroid of same mass and rigidity, with radius equal to the volume equivalent radius (R_V≈59.1 km). For the spherical body, the dissipated power is given as (e., g., Murray and Dermott, 1999, pp. 162-164) :

$$\dot{E}_{Sphere} = \frac{3}{2}\left(\frac{k_2}{Q}\right)\frac{Gm_2^2}{a_2^6}R_V^5(\Omega - n_2) \qquad (57)$$

where k_2 is given by equation (1).

For each value of the asteroid length 2L, the rate of tidal energy dissipation $\dot{E}_T$ (including bending and compressional tides) was computed through our dumbbell model, from which the dissipation ratio $\delta=\dot{E}_T/\dot{E}_{Sphere}$ was deduced. Here, in contrast to what has been done so far, the compressional tide along the y direction (see section 3.2) can no more be neglected for poorly elongated bodies, and therefore the compressional tide here includes both tides along x and along y. The result, given here assuming Q=40, is displayed in **Figure 8.** It can be seen that for 2L≈102km (corresponding to λ=(B-A)/C≈0 from **Figure 7),** the dissipation ratio δ is ≈25% lower than the expected value δ=1. This difference may be explained notably by the fact that our tidal dissipation model becomes inadequate when λ<<1. In particular, under an acceleration (say Γ_x along the x direction), only the motion of the rod in the longitudinal direction was considered. However there is some lateral motion because longitudinal stresses induce lateral strains. This effect has been ignored because it has a minor effect if the rod is fairly long compared to its diameter (Stokey, 2002), which is the case for Kleopatra. Therefore our modeled tidal dissipation should be regarded as an underestimate for λ<<1.

As the asteroid length 2L increases, our modeled dissipation ratio increases dramatically. In **Figure 8,** for the situation of Kleopatra (2L=267km, corresponding to λ=0.896), the dissipation ratio is as high as δ≈240. The tidal behaviour of the elongated asteroid thus differs considerably from what would be expected from a spherical asteroid.

Note that the shape of the asteroid has a great importance too : if instead of taking the dumbbell geometry we used the cylindrical model, the dissipation ratio for Kleopatra (λ=0.893 in that case) would drop to δ≈111. If ever we had modeled the asteroid as an axisymmetric ellipsoid with axis of symmetry along Ox, with the same material properties (density, rigidity) as taken here, same mass, same length (major axis of the ellipsoid 2L=267km), the dissipation ratio for Kleopatra (λ≈0.840 in that case) would be no higher than δ≈14. For elongated objects with ellipsoidal shape, such as dwarf planet Haumea (Dunham et al., 2019), the effect of shape on tidal dissipation is therefore expected to be significantly less pronounced than it is for Kleopatra.

7.4. Kleopatra's rigidity within the hypothesis of a 3:2 mean motion resonance between both satellites

So far in this paper we have assumed that one can ignore the effect of the inner satellite when interpreting the measured $\dot{P}_2$, as discussed in section 2 above. This assumption would be invalidated if both satellites were trapped in a mean motion resonance. The ratio between orbital periods, $P_2/P_1 \approx 1.507$, is close to the the 3:2 mean motion resonance. However, Broz et al.'s (2021) numerical tests tended to show that the critical angle of the 3:2 mean motion resonance do not librate, because orbits are much perturbed by the multipoles of Kleopatra and eccentricities are too small, and thus no secular interaction between both satellites is expected. Nevertheless, recognizing that a resonant locking should not be completely excluded as long as no direct measurement of the migration rate $\dot{P}_1$ has been done, Broz et al. (2022) explored an alternative model with moons captured in a 3:2 mean motion resonance. If that situation were occurring, the tides acting on the first moon would also act on the second moon, due to the new constraint $\dot{P}_2 = 1.5\dot{P}_1$, and they conclude that a lower dissipation in Kleopatra would be sufficient to explain the observed $\dot{P}_2$. According to their numerical experiment, the inferred value Q/k_2 entering in our equation (57) would increase from Q/k_2=131 for the non-resonant case to Q/k_2=250 in the resonant case. From equation (57), it is seen that the dissipated power within the asteroid is proportional to k_2/Q, and the same is true for the period rate $\dot{P}_2$. This implies that, of the observed period rate $\dot{P}_2$ of satellite 2, only a fraction $\dot{P}_2'$=131/250$\dot{P}_2$=0.56$\dot{P}_2$ is due to the tidal effect of satellite 2, the other part being an indirect effect of satellite 1 due to resonance locking. In **Figure 5**, the measured period rate $\dot{P}_2$=1.8x10^{-8} day/day represented by the horizontal line should then be replaced by the amount really due to tides raised by satellite 2, $\dot{P}_2'$ ≈1.0x10^{-8} day/day. In the case of **Figure 5** (where Q=40 was assumed), the material rigidity μ for which the computed period rate matches $\dot{P}_2'$ becomes μ≈2.52x10^7 Pa in the resonant case (instead of 1.94x10^7 Pa for the non-resonant case), which corresponds to a 30% increase. If Q=100 were assumed, then the inferred rigidity would also increase from μ≈1.40x10^7 Pa (non-resonant case) to μ≈1.7x10^7 Pa (resonant case), which corresponds to a 21% increase.

8. Conclusion

The classical theory of planetary tidal dissipation is usually given for spherical or near spherical planets (Goldreich and Sari, 2009). Although such an approach is most often fully appropriate, it may become irrelevant for exotic planetary bodies whose shapes deviate significantly from a sphere. This is the case for some highly elongated asteroids, among which asteroid (216)Kleopatra is exemplary. The aim of this paper was to compute the tidal dissipation within such highly elongated asteroids. Here the asteroid is modeled as an homogeneous beam (or rod) whose shape is either cylindrical, or, more realistically, dumbbell shaped. The asteroid is spinning rapidly (spin period 5.38 hours for Kleopatra). The first effect of the tidal force exerted by the satellite is to superimpose a libration to the asteroid's spin. This libration raises inertial and Coriolis acceleration in the asteroid's body (librating) frame. Due to elasticity of the asteroid, the stresses produced within the body rise a compression tide in the direction of the asteroid's long axis, and a bending tide in the perpendicular direction. We computed the tidal amplitude of the total elastic energy stored within the asteroid, as a function of Young's modulus E. Provided that the tidal quality factor Q is known, this permits to deduce the power tidally dissipated within the asteroid. This computed dissipated power is compared to the measured tidal dissipation, which has been obtained by Broz et al.'s (2022) observations of the tidal migration of Kleopatra's outer satellite. This permits to deduce the asteroid's Young's modulus E (or equivalently the rigidity μ through μ≈E/(2.6±0.1)).

Assuming a quality factor Q≈40, we obtained here a rigidity $\mu \approx 1.94 \times 10^7$ Pa for Kleopatra. If one takes Q=100, the inferred rigidity is reduced to $\mu \approx 1.40 \times 10^7$ Pa. Those situations are found to be far away from resonance for the bending tide ($\omega_S/\omega_{OB} \approx 0.205$) and reasonably far from resonance for the compressional tide ($\omega_S/\omega_{Ox} \approx 0.476$) where ω_S is the semi-diurnal tidal angular frequency and ω_{OB} and ω_{Ox} are the fundamental resonance angular frequencies of the bending and compressional tides. Compared to Marchis et al.'s(2008) estimate $\mu Q \approx 10^{10}$ Pa, our inferred value is 7 to 13 times lower than the value they proposed.

The dissipated power computed here was compared to the power dissipated within an hypothetical spherical asteroid of same mass and rigidity as Kleopatra, with radius equal to the volume equivalent radius ($R_V \approx 59.1$ km). We defined the dissipation ratio δ as the ratio between the tidally dissipated power within Kleopatra, and within such equivalent spherical body. For our dumbbell model with Q=40, we found δ≈240. For the cylindrical model with same length of long axis (2L=267km), we found δ≈111. Finally, for an axisymmetric ellipsoid in the same conditions, we would have obtained δ≈14. One concludes that (i) the tidal dissipation is strongly dependent upon the shape of the asteroid, and (ii) for the dumbbell model the tidal dissipation is more than 2 orders of magnitude higher than for the equivalent spherical body.

This work was done assuming that the asteroid may be regarded as an elastic solid. However we are dealing here with a body that is not really solid, but rather a weak medium presumably made up of rubble pile. Dissipation in these weak media is not determined by their rigidity, but rather by their viscosity (Efroimsky, 2015). A more realistic approach would be to represent the asteroid as a viscoelastic body, which behaves like a solid at high frequencies and like a fluid at low frequencies. Considering the asteroid as an elastic solid is however justified under to two conditions: (i) the asteroid is made of a Maxwell material and (ii) the frequencies are greater than the inverse of Maxwell time. For a Maxwell body, the phase lag δ(ω) between stress and strain at angular frequency ω verifies

$$tan(\delta(\omega)) = (\omega\tau_M)^{-1} \qquad (58)$$

where the Maxwell time τ_M is the ratio between viscosity η and rigidity μ ($\tau_M = \eta/\mu$) (Efroimsky, 2012). In this paper the forcing angular frequency ω is the semi-diurnal frequency ω_S, and we assumed either Q=40 or Q=100, and therefore Q>>1 . Since the quality factor may also be written $Q^{-1} = sin|\delta|$, it follows that δ<<1, and therefore, from equation (58), $\omega\tau_M \gg 1$ and $Q^{-1} \approx (\omega\tau_M)^{-1}$ to second order in δ. Since $\tau_M = \eta/\mu$, one gets $\mu Q \approx \omega\eta$. This is the situation where the forcing frequency ω is much greater than the inverse of Maxwell time. Thus, the approach of considering the asteroid as an elastic solid is consistent, provided that we note that the inferred μQ is actually ωη.

APPENDIX A: Energy stored in a forced harmonic oscillator:

Here we recall the effect of resonance on the elastic energy stored in a forced harmonic oscillator, which is materialized here as a mass m hanging from a simple spring. The differential equation describing the forced oscillation of the abscissa x of the mass may be written, classically:

$$\ddot{x} + \frac{\omega_O}{Q}\dot{x} + \omega_O^2 x = \frac{F_E}{m}\cos(\omega_S t) \quad \text{(A1)}$$

where Q is quality factor, F_E is the amplitude of the external sinusoidal force, ω_O is the natural angular frequency of the oscillator ($\omega_O = \sqrt{k/m}$ where k is the spring constant), and ω_S is the forcing angular frequency. Looking for solutions in the form $x(t) = Xcos(\omega_S t + \varphi)$, we replace x by the complex variable $\hat{x} = Xexp\, i(\omega_S t + \varphi)$, so that equation (A1) becomes:

$$-\omega_S^2\hat{x} + \frac{\omega_O}{Q} i\omega_S\hat{x} + \omega_O^2\hat{x} = \frac{F_E}{m}\exp(i\omega_S t) \quad \text{(A2)}$$

Solving for $\hat{x}$, one gets:

$$\hat{x} = \frac{F_E}{m}\ \frac{\exp(i\omega_S t)}{\omega_O^2 - \omega_S^2 + i\frac{\omega_S\omega_O}{Q}} \quad \text{(A3)}$$

whose modulus may thus be written:

$$|\hat{x}| = \frac{F_E}{m\omega_O^2\sqrt{(1-\eta^2)^2 + \frac{\eta^2}{Q^2}}} \quad ; \quad where \quad \eta = \frac{\omega_S}{\omega_O} \quad \text{(A4)}$$

The static case may be obtained by simply stating $\omega_S = 0$. This gives $\eta = 0$, and from equation (A3), $\hat{x} = F_E/(m\omega_O^2)$ in the static case.

The elastic energy stored in the oscillator is proportional to the square of amplitude of displacement. Thus from equation (A4), the amplitude of the energy stored in the forced oscillator with a forcing frequency $\omega_S = \eta\omega_O$, is equal to the energy stored in the static case multiplied by the following resonance factor:

$$K(\eta) = \frac{1}{(1-\eta^2)^2 + \frac{\eta^2}{Q^2}} \quad \text{(A5)}$$

Table 1. Physical characteristics of the Kleopatra system.

870 Characteristics of main body are from Marchis et al. (2021) MCPD shape model. Characteristics of both satellites are from Broz et al. (2021) best fit model and Broz et al. (2022).

Main body	**Symbol**	**Value**
mass	M	2.97×10^{18} kg
density	ρ	3430 kg/m^3
volume equivalent radius	$R_V=(3M/4\pi\rho)^{1/3}$	59.1 km
length of axis a	a=2L	267 km
sidereal spin period	P	5.385 hours
sidereal spin angular frequency	$\Omega=2\pi/P$	3.241×10^{-4} rad/s
Elliptical cylinder model:		
average cross section area	$S=M/(2L\rho)$	3240 km^2
ratio R_y/R_z	σ_o	1.3
radius along y	$R_y = \sqrt{\sigma_O S/\pi}$	36.6 km
radius along z	$R_z = \sqrt{S/\sigma_O \pi}$	28.2 km
Dumbbell model: modulation of R_y and R_z: $R_y = R_{yO}\left[1-\varepsilon\left\{1+cos\left(\frac{3\pi}{2}\frac{x}{L}\right)\right\}\right]$; $R_z = R_{zO}\left[1-\varepsilon\left\{1+cos\left(\frac{3\pi}{2}\frac{x}{L}\right)\right\}\right]$		
modulation coefficient	ε	0.13
reference radius in y direction	R_{yO}	40.6 km
reference radius in z direction	R_{zO}	31.2 km
Inner satellite:		
mass	m_1	4×10^{14} kg
semi-major axis	a_1	499 km
orbital period	P_1	1.822 day
Outer satellite:		
mass	m_2	6×10^{14} kg
semi-major axis	a_2	655 km
orbital period	P_2	2.746 days
mean motion	$n_2=2\pi/P_2$	2.648×10^{-5} rad/s
orbital period variation rate	$\dot{P}_2$	$(1.8\pm0.1) \times 10^{-8}$ day day^{-1}
semi-diurnal tidal angular frequency	$\omega_S=2(\Omega-n_2)$	5.952×10^{-4} rad/s

875

REFERENCES

Broz, M., Marchis, F., Jorda, L., and 37 authors, 2021. An advanced multipole model for (216) Kleopatra triple system. *Astronomy and Astrophysics, 653*, A56 (9 pp.).

880

Broz, M., Durech, J., Carry, B., Vachier, F., Marchis, F., Hanus, J., Jorda, L., Vernazza, P., Vokrouhlicky, D., Walterova, M., and Behrend, R., 2022. Observed tidal evolution of Kleopatra's outer satellite. *Astronomy and Astrophysics, 657*, A76.

885 Davy, P., Darcel, C., Le Goc, R., and Mas Ivars, D., 2018. Elastic properties of fractured rock masses with frictional properties and power law fracture size distributions. *J. Geophys. Res. : Solid Earth, 123*,6521-6539.

Descamps, P., 2015. Dumb-bell-shaped equilibrium figures for fiducial contact-binary
890 asteroids and EKBOs. *Icarus, 245,* 64-79.

Descamps, P., 2016. Near-equilibrium dumb-bell-shaped figures for cohesionless small bodies. *Icarus, 265,* 29-34.

895 Dunham, E. T., Desch, S. J., and Probst, L., 2019. Haumea's shape, composition, and internal structure. *The Astrophysical Journal, 877:41* (11 pp).

Efroimsky, M., 2012. Tidal dissipation compared to seismic dissipation: in small bodies, Earths, and super-Earths. *The Astrophysical Journal, 746:150* (20 pp).

900

Efroimsky, M., 2015. Tidal evolution of asteroidal binaries. Ruled by viscosity. Ignorant of rigidity. *The Astrophysical Journal, 150:98* (12 pp).

Goldreich, P., and Peale, S., 1966. Spin-orbit coupling in the solar system. *The Astronomical*
905 *Journal, 71 (6),* 425-437.

Goldreich, P., and Sari, R., 2009. Tidal evolution of rubble piles. *The Astrophysical Journal, 691,* 54-60.

910 Marchis, F., Descamps, P., Baek, M., Harris, A. W., Kaasalainen, M., Berthier, J., Hestroffer, D., and Vachier, F., 2008. Main belt binary asteroidal systems with circular mutual orbits. *Icarus, 196,* 97-118.

Marchis, F., Jorda, L., Vernazza, P., and 36 authors, 2021. (216) Kleopatra, a low density
915 critically rotating M-type asteroid. *Astronomy and Astrophysics, 653*, A57.

Murray, C. D., and Dermott, S. F., 1999. *Solar System Dynamics,* Cambridge University Press, New York.

920 Scheeres, D. J., Hartzell, C. M., Sanchez, P., and Swift, M., 2010. Scaling forces to asteroid surfaces: The role of cohesion. *Icarus, 210,* 968-984.

Slaughter, W. S., 2002. *The Linearized Theory of elasticity*. Chapter 1, Birkhäuser, Boston.

925 Stokey W. F., 2002. Vibration of systems having distributed mass and elasticity, in *Harris' shock and vibration handbook,* chapter 7, C. M. Harris and A. G. Piersol editors, 5th ed ., McGraw-Hill, New York.

Figure captions

Figure 1.
Model shape of the asteroid (216) Kleopatra taken in the dumbbell model. Upper panel : view from above ; lower right panel : side view from axis y ; left panel : view from axis Ox. Parameters chosen for the model are given in **Table 1**.

Figure 2.
Schematic view of the asteroid (here modeled as a cylinder) with its satellite (view from above). The satellite is assumed to be rotating in a circular orbit in the $(\overrightarrow{Ox}, \overrightarrow{Oy})$ plane. The angle $\chi' = \chi - \xi$ is the satellite azimuth in the body frame.

Figure 3.
Ratio $q=E_{Sy}/E_{Sx}$ between the compressional strain energies E_{Sy} and E_{Sx} stored in the y and x directions, respectively (solid line for dumbbell model, dashed line for cylindrical model). The ratio was computed for model asteroids with the same mass and density as Kleopatra, but with the asteroid length 2L along the x axis taken as a free parameter (the radii R_{yO} and R_{zO} are modified accordingly to preserve volume). The result is plotted as a function of the triaxiality $\lambda=(B-A)/C$ of the asteroid. The vertical dotted line indicates the actual value (B-A)/C = 0.896 of asteroid Kleopatra in our dumbbell model.

Figure 4.
Sketch illustrating the bending moment produced about the axis parallel to $\overrightarrow{Oz}$ that passes through point Q located on the x axis, by a force $\vec{F}$ acting at point A (see text).

Figure 5.
Computed migration period rate $\dot{P}_2$, as a function of assumed material rigidity μ of the asteroid for the dumbbell model. Here a quality factor Q=40 is taken. Dashed line : contribution from the compressional tide. Dotted line : contribution from the bending tide. Solid line : total computed period rate. The thin horizontal line is the period rate measured by Broz et al. (2022) ($\dot{P}_2=1.8\text{x}10^{-8}$ day/day). The rigidity for which computed and measured period rates are equal is $\mu=1.94\text{x}10^7$ Pa.

Figure 6.
Maximum values of the distortions h_x and h_B, defined in equation (52), as a function of distance along x axis, for the dumbbell model. Solid line : bending distortion h_B, attained for $\chi=-45°$; the curve also represents the shape of the distorted longitudinal axis of the asteroid, with coordinate y magnified by a factor of about $2.5\text{x}10^6$. Dashed line : compressional distortion, attained for $\chi=0°$. A quality factor Q=40 is assumed for the asteroid, implying a rigidity $\mu=1.94\text{x}10^7$ Pa to be consistent with Broz et al.'s (2022) observation of the migration period rate $\dot{P}_2$.

Figure 7.
Triaxiality $\lambda=(B-A)/C$ as a function of asteroid length 2L. Solid line is obtained with the dumbbell model, and dashed line is obtained with the cylinder model. The vertical dotted line indicates the situation of Kleopatra (2L=267km).

Figure 8.

Ratio $\delta=\dot{E}_T/\dot{E}_{Sphere}$ between the computed tidal dissipation within a dumbbell asteroid and within a spherical asteroid with same mass and volume. The ratio δ is plotted as a function of the asteroid length 2L. Quality factor Q=40 and rigidity $\mu=1.94\text{x}10^7$ Pa are assumed. Solid line : total tidal dissipated power. Dashed line : power dissipated by compressional tides alone (including x and y directions). Dotted line : Power dissipated by bending tide alone. The vertical dotted line indicates the situation of Kleopatra (2L=267km, corresponding to $\lambda=0.896$).

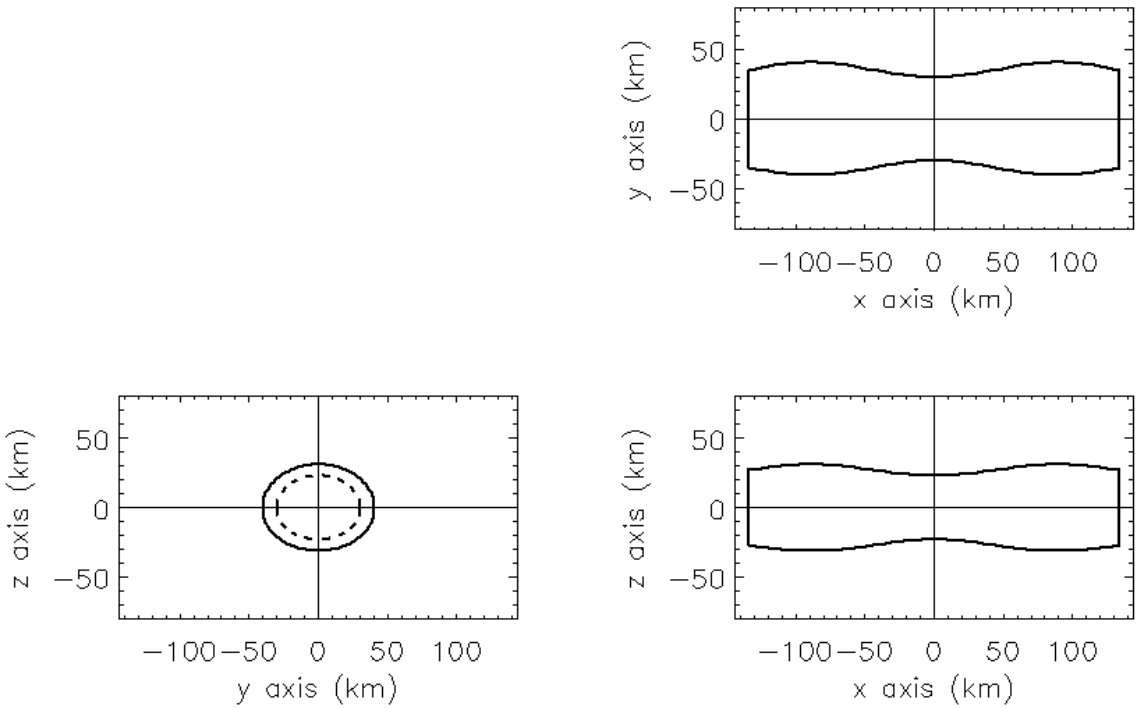

Figure 1.
Model shape of the asteroid (216) Kleopatra taken in the dumbbell model. Upper panel : view from above ; lower right panel : side view from axis y ; left panel : view from axis Ox. Parameters chosen for the model are given in **Table 1**.

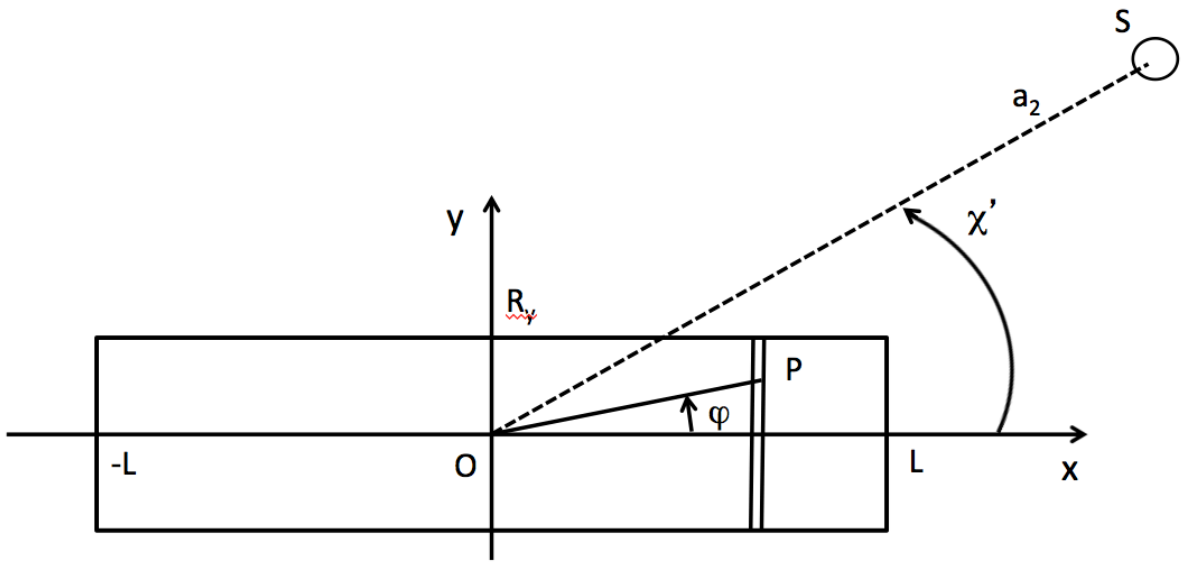

Figure 2.
Schematic view of the asteroid (here modeled as a cylinder) with its satellite (view from above). The satellite is assumed to be rotating in a circular orbit in the $(\overrightarrow{Ox}, \overrightarrow{Oy})$ plane. The angle $\chi' = \chi - \xi$ is the satellite azimuth in the body frame.

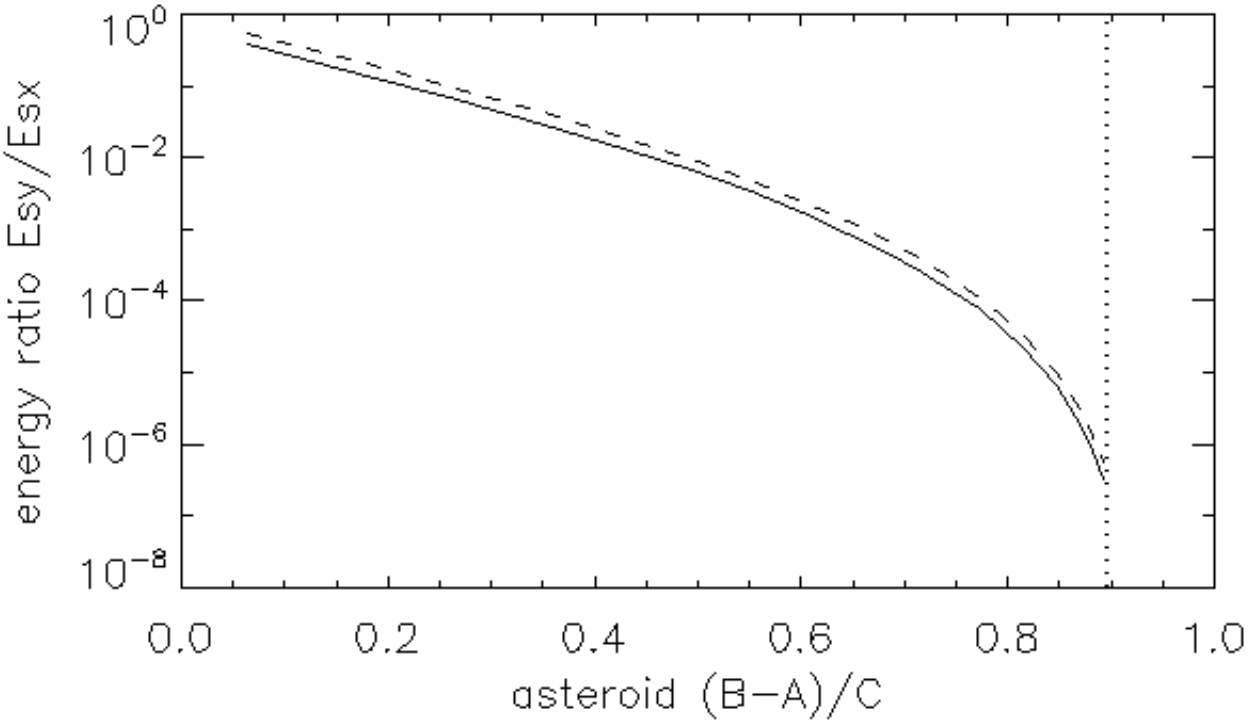

Figure 3.

Ratio $q=E_{Sy}/E_{Sx}$ between the compressional strain energies E_{Sy} and E_{Sx} stored in the y and x directions, respectively (solid line for dumbbell model, dashed line for cylindrical model). The ratio was computed for model asteroids with the same mass and density as Kleopatra, but with the asteroid length 2L along the x axis taken as a free parameter (the radii R_{yO} and R_{zO} are modified accordingly to preserve volume). The result is plotted as a function of the triaxiality $\lambda=(B-A)/C$ of the asteroid. The vertical dotted line indicates the actual value (B-A)/C = 0.896 of asteroid Kleopatra in our dumbbell model.

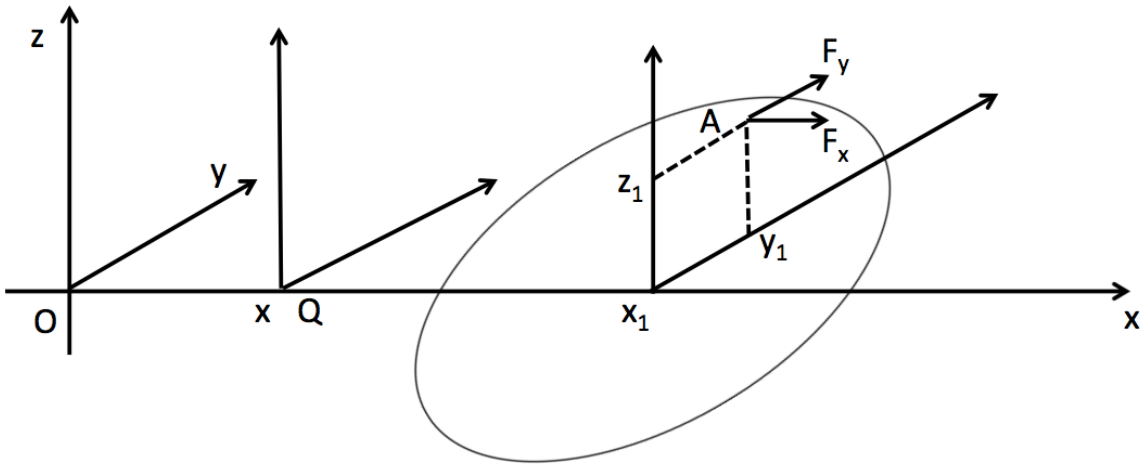

Figure 4.

Sketch illustrating the bending moment produced about the axis parallel to $\overrightarrow{Oz}$ that passes through point Q located on the x axis, by a force $\vec{F}$ acting at point A (see text).

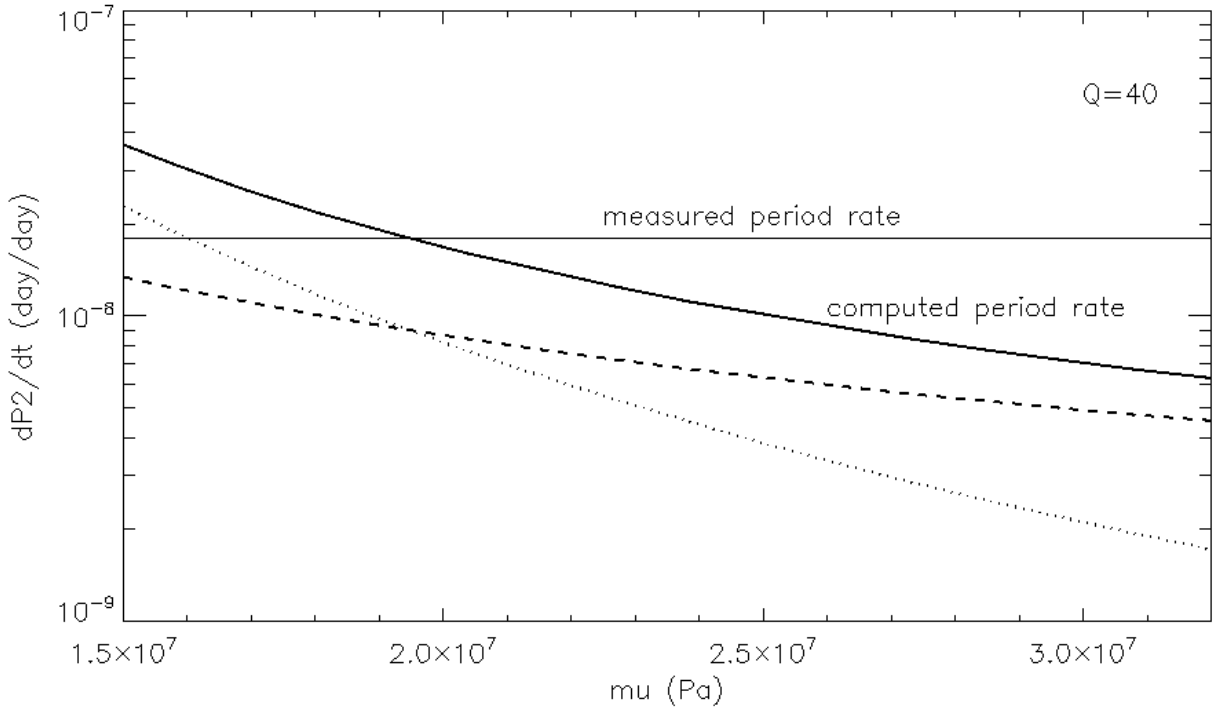

Figure 5.

Computed migration period rate $\dot{P}_2$, as a function of assumed material rigidity μ of the asteroid for the dumbbell model. Here a quality factor Q=40 is taken. Dashed line : contribution from the compressional tide. Dotted line : contribution from the bending tide. Solid line : total computed period rate. The thin horizontal line is the period rate measured by Broz et al. (2022) ($\dot{P}_2$=1.8x10^{-8} day/day). The rigidity for which computed and measured period rates are equal is μ=1.94x10^7 Pa.

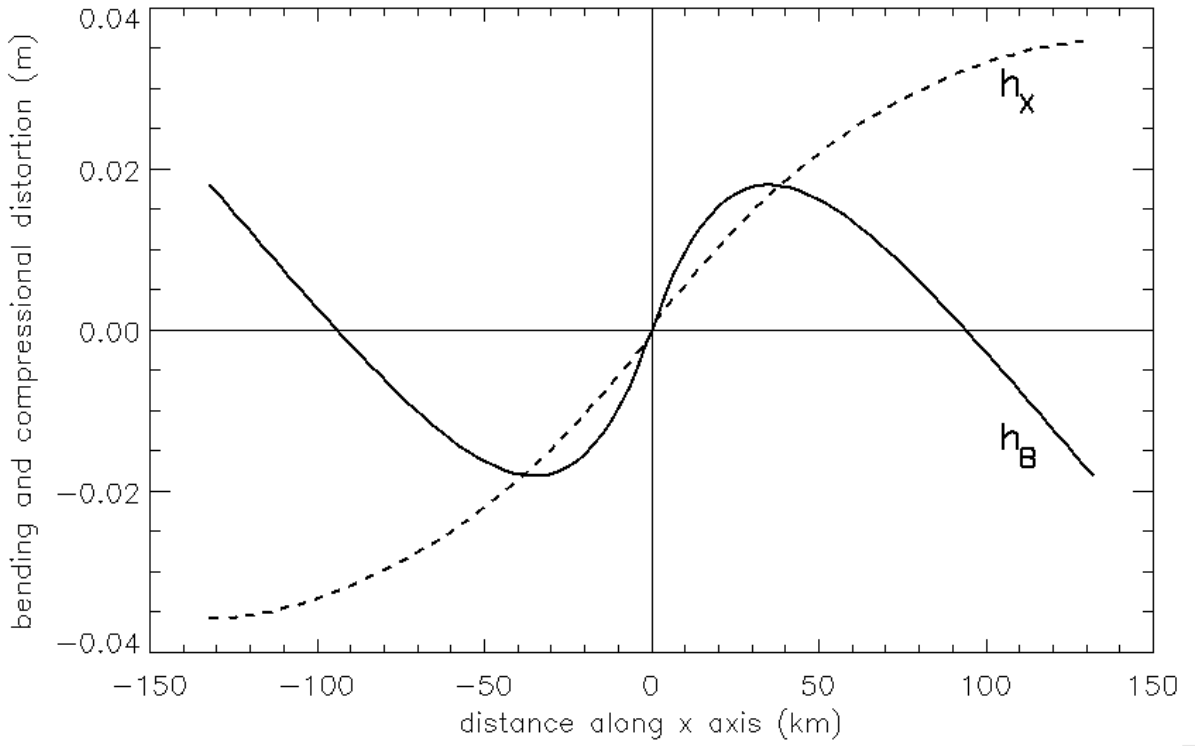

Figure 6.

Maximum values of the distortions h_x and h_B, defined in equation (52), as a function of distance along x axis, for the dumbbell model. Solid line : bending distortion h_B, attained for χ=-45° ; the curve also represents the shape of the distorted longitudinal axis of the asteroid, with coordinate y magnified by a factor of about 2.5×10^6. Dashed line : compressional distortion, attained for χ=0°. A quality factor Q=40 is assumed for the asteroid, implying a rigidity $\mu = 1.94 \times 10^7$ Pa to be consistent with Broz et al.'s (2022) observation of the migration period rate $\dot{P}_2$.

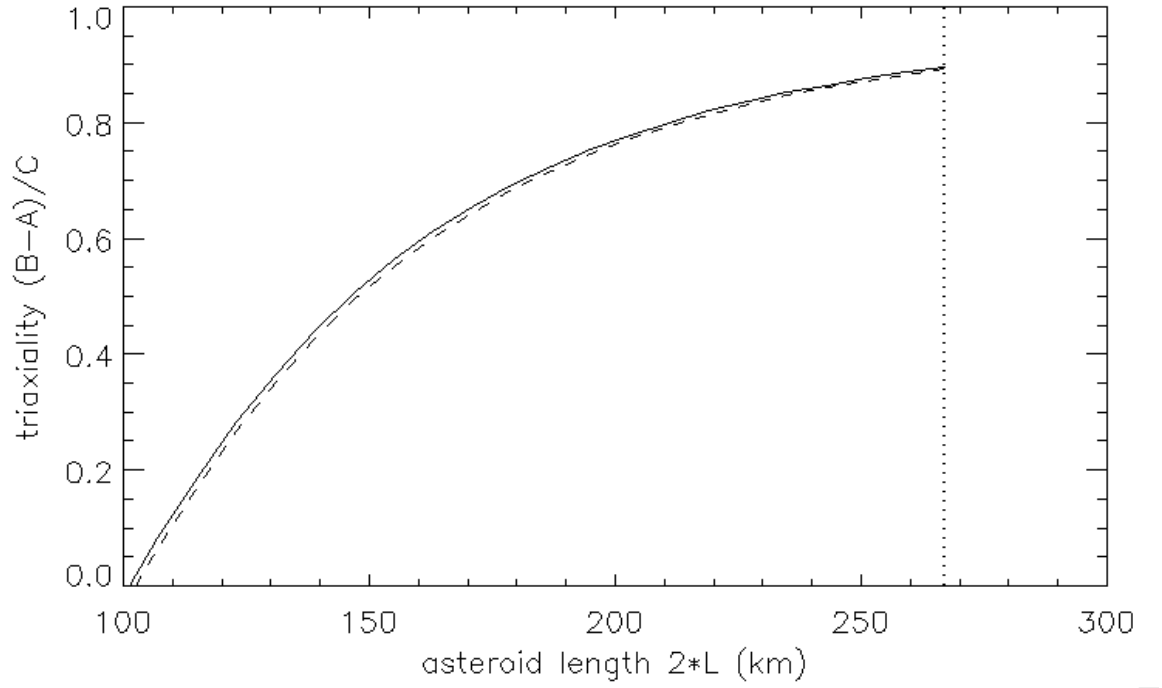

1105

1110 **Figure 7.**

Triaxiality λ=(B-A)/C as a function of asteroid length 2L. Solid line is obtained with the dumbbell model, and dashed line is obtained with the cylinder model. The vertical dotted line indicates the situation of Kleopatra (2L=267km).

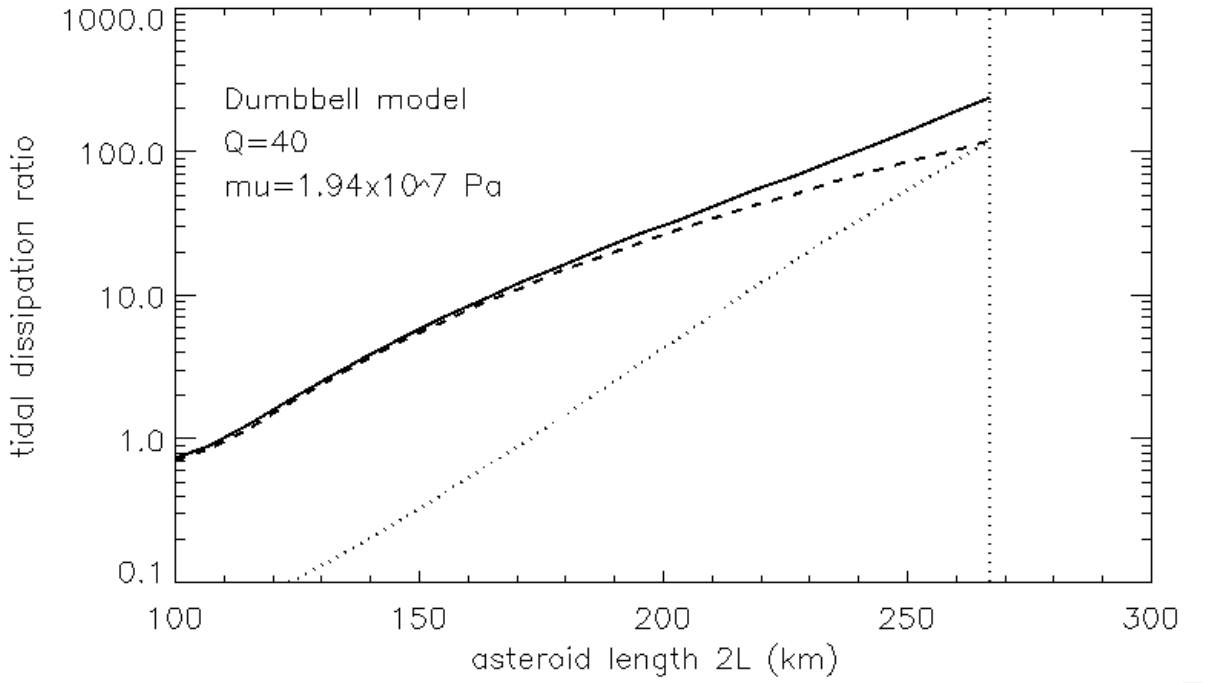

Figure 8.

Ratio $\delta=\dot{E}_T/\dot{E}_{Sphere}$ between the computed tidal dissipation within a dumbbell asteroid and within a spherical asteroid with same mass and volume. The ratio δ is plotted as a function of the asteroid length 2L. Quality factor Q=40 and rigidity $\mu=1.94\text{x}10^7$ Pa are assumed. Solid line : total tidal dissipated power. Dashed line : power dissipated by compressional tides alone (including x and y directions). Dotted line : Power dissipated by bending tide alone. The vertical dotted line indicates the situation of Kleopatra (2L=267km, corresponding to λ=0.896).